THE JOURNAL OF PHYSICAL CHEMISTRY A

Article

pubs.acs.org/JPCA

Stochastic Optimally Tuned Range-Separated Hybrid Density Functional Theory

Daniel Neuhauser,[*,†] Eran Rabani,[*,‡,⊥,¶] Yael Cytter,[§] and Roi Baer[*,§,∥]

[†]Department of Chemistry and Biochemistry, University of California at Los Angeles, Los Angeles, California 90095 United States
[‡]Department of Chemistry, University of California, Berkeley, California 94720, United States
[⊥]Materials Science Division, Lawrence Berkeley National Laboratory, Berkeley, California 94720, United States
[¶]The Sackler Center for Computational Molecular and Materials Science, Tel Aviv University, Tel Aviv, Israel 69978
[§]Fritz Haber Center for Molecular Dynamics, Institute of Chemistry, The Hebrew University of Jerusalem, Jerusalem 91904, Israel

ABSTRACT: We develop a stochastic formulation of the optimally tuned range-separated hybrid density functional theory that enables significant reduction of the computational effort and scaling of the nonlocal exchange operator at the price of introducing a controllable statistical error. Our method is based on stochastic representations of the Coulomb convolution integral and of the generalized Kohn−Sham density matrix. The computational cost of the approach is similar to that of usual Kohn−Sham density functional theory, yet it provides a much more accurate description of the quasiparticle energies for the frontier orbitals. This is illustrated for a series of silicon nanocrystals up to sizes exceeding 3000 electrons. Comparison with the stochastic GW many-body perturbation technique indicates excellent agreement for the fundamental band gap energies, good agreement for the band edge quasiparticle excitations, and very low statistical errors in the total energy for large systems. The present approach has a major advantage over one-shot GW by providing a self-consistent Hamiltonian that is central for additional postprocessing, for example, in the stochastic Bethe−Salpeter approach.

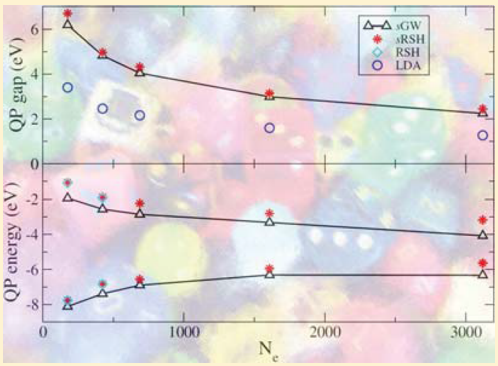

INTRODUCTION

First-principles descriptions of quasiparticle excitations in extended and large confined molecular systems are prerequisite for understanding, developing, and controlling molecular electronic, optoelectronic, and light-harvesting devices. In search of reliable theoretical frameworks, it is tempting to use Kohn−Sham density functional theory (KS-DFT),[1] which provides accurate predictions of the structure and properties of molecular, nanocrystal (NC), and solid-state systems. However, KS-DFT approximations poorly predict quasiparticle excitation energies in both confined and extended systems,[2−4] even for the frontier occupied orbital energy, for which KS-DFT is expected to be exact.[5−7] This has led to the development of two main first-principles alternative frameworks for quasiparticle excitations. The first is the GW approximation,[8] providing a self-energy for the single-particle equations for the Dyson orbitals[9] and often applied as a perturbative correction over KS-DFT (the so-called G_0W_0 approximation).[10] This approach provides estimates of quasiparticle energies and quasiparticle gaps that are close to experimental results.[11−25]

A different route for quasiparticle energies invokes generalized KS-DFT approaches,[26−30] and in the present paper, we concentrate on the long-range separated hybrid (RSH) functionals[31−37] combined with an optimally tuned range parameter.[38,39] This approach provides quantitative predictions of quasiparticle band gaps, band edge energies, and excitation energies for a range of interesting *small* molecular systems, matching well both experimental results and GW predictions.[40−43] The key element of the range parameter tuning is the minimization of the deviation between the highest occupied orbital energy and the ionization energy[39,40] or the direct minimization of the energy curvature.[44]

The use of GW and the optimally tuned RSH (OT-RSH) approaches for describing quasiparticle excitations in *extended* systems is hampered by high computational scaling. The computational bottleneck in GW is in the calculation of the screened potential within the Random Phase Approximation (RPA), while in OT-RSH, it is the application of nonlocal exchange to each of the molecular orbitals. OT-RSH is a self-consistent method and should therefore be compared to self-consistent GW calculations; however, the latter are extremely expensive as the self-energy operator must be applied repeatedly to all Dyson orbitals.

Recently, we proposed a stochastic formulation limited to the G_0W_0 approach, where the computational complexity was reduced by combining stochastic decomposition techniques

Special Issue: Ronnie Kosloff Festschrift

Received: October 28, 2015
Revised: December 9, 2015

DOI: 10.1021/acs.jpca.5b10573
J. Phys. Chem. A XXXX, XXX, XXX−XXX

and real-time propagation to obtain the expectation value of the self-energy within the GW approximation.[45] The stochastic GW (sGW) was used to describe quasiparticle energies in very large silicon NCs with $N_e > 3000$ (N_e is the number of electrons), with computational complexity scaling nearly linearly with the system size. Similar stochastic techniques have been developed by us for DFT,[46] for embedded DFT,[47] and for other electronic structure problems.[48−52]

Here, we develop a stochastic formalism suitable for applying the OT-RSH functionals for studying quasiparticle excitations in extended systems. The approach builds on our previous experience with the exchange operator,[53−55] but several new necessary concepts are developed here for the first time. We start with a brief review of the OT-RSH approach, then move on to describe the specific elements of the stochastic approach, and finally present results.

OPTIMALLY TUNED RANGE-SEPARATED HYBRID FUNCTIONALS

For a systems of N_e electrons in an external one-electron potential $\nu_{ext}(\mathbf{r})$ having a total spin magnetization s_z in the z direction, the OT-RSH energy is a functional of the spin-dependent density matrix (DM) $\rho_{\uparrow,\downarrow}(\mathbf{r},\mathbf{r}')$ given in atomic units as

$$E^{\gamma}_{RSH}[\rho_\uparrow, \rho_\downarrow] = \mathrm{Tr}\left[\rho\left(-\frac{1}{2}\hat{\nabla}^2 + \nu_{ext}(\hat{\mathbf{r}})\right)\right] + E_H[n] + E^{\gamma}_{XC}[n] + K^{\gamma}_X[\rho_\uparrow, \rho_\downarrow], \quad (1)$$

where γ is the range parameter, discussed below, while

$$E_H[n] = \frac{1}{2}\iint u_C(|\mathbf{r} - \mathbf{r}'|)n(\mathbf{r})n(\mathbf{r}')\,d\mathbf{r}\,d\mathbf{r}', \quad (2)$$

is the Hartree energy functional of the density $n(\mathbf{r}) = \rho(\mathbf{r},\mathbf{r}) = \sum_{\sigma=\uparrow\downarrow}\rho_\sigma(\mathbf{r},\mathbf{r})$ and $u_C(r) = r^{-1}$ is the Coulomb potential energy. $E^{\gamma}_{XC}[n]$ is the unknown γ-dependent exchange−correlation energy functional, which in practical applications is approximated. The nonlocal exchange energy functional is given by

$$K^{\gamma}_X[\rho_\uparrow, \rho_\downarrow] = -\frac{1}{2}\sum_{\sigma=\uparrow,\downarrow}\iint u^{\gamma}_C(|\mathbf{r} - \mathbf{r}'|)|\rho_\sigma(\mathbf{r}, \mathbf{r}')|^2\,d\mathbf{r}\,d\mathbf{r}', \quad (3)$$

where $u^{\gamma}_C(r) = r^{-1}\,\mathrm{erf}(\gamma r)$. This choice of $u^{\gamma}_C(r)$ accounts for long-range contributions to the nonlocal exchange energy and thus dictates a complementary cutoff in the approximate *local* exchange−correlation energy, $E^{\gamma}_{XC}[n]$, to avoid overcounting the exchange energy.[32,39,56]

When the exact $E^{\gamma}_{XC}[n]$ functional is used, minimizing $E^{\gamma}_{RSH}[\rho_\uparrow,\rho_\downarrow]$ with respect to $\rho_\sigma(\mathbf{r},\mathbf{r}')$ under the constraints specified below leads to the exact ground-state energy and electron density $n(\mathbf{r})$. For approximate $E^{\gamma}_{XC}[n]$, approximate estimates of these quantities are obtained. To express the constraints, we first require the spin-dependent DM to be Hermitian and thus expressible as

$$\rho_\sigma(\mathbf{r}, \mathbf{r}') = \sum_j f_{j,\sigma}\phi_{j,\sigma}(\mathbf{r})\phi^*_{j,\sigma}(\mathbf{r}'), \quad (4)$$

where $f_{j,\sigma}$ and $\phi_{j,\sigma}(\mathbf{r})$ are its eigenvalues and orthonormal eigenfunctions. The constraints are then given in terms of the eigenvalues $f_{j\sigma}$ as

$$0 \le f_{j,\sigma} \le 1 \quad (5)$$

$$\sum_{j,\sigma} f_{j,\sigma} = N_e \quad (6)$$

$$\frac{1}{2}\sum_j (f_{j,\uparrow} - f_{j,\downarrow}) = s_z. \quad (7)$$

The necessary conditions for a minimum of $E^{\gamma}_{RSH}[\rho_\uparrow,\rho_\downarrow]$ is that $\phi_{j,\sigma}(\mathbf{r})$ obey the generalized KS equations

$$\hat{h}^{\gamma}_\sigma\phi^{\gamma}_{j,\sigma}(\mathbf{r}) = \varepsilon^{\gamma}_{j,\sigma}\phi^{\gamma}_{j,\sigma}(\mathbf{r}), \quad (8)$$

where $\varepsilon^{\gamma}_{j,\sigma}$ are the spin-dependent eigenvalues of the generalized KS Hamiltonian (j = 1, 2, ... and $\sigma = \uparrow\downarrow$) given by

$$\hat{h}^{\gamma}_\sigma = -\frac{1}{2}\hat{\nabla}^2 + \nu^{\gamma}_\sigma(\hat{\mathbf{r}}) + \hat{k}^{\gamma}_\sigma. \quad (9)$$

Note that the DM and its eigenstates minimizing the energy functional $E^{\gamma}_{RSH}[\rho_\uparrow,\rho_\downarrow]$ are themselves γ-dependent and are thus denoted by $\rho^{\gamma}_\sigma(\mathbf{r},\mathbf{r}')$, $\phi^{\gamma}_{j,\sigma}(\mathbf{r})$; the DM eigenvalues are not γ-dependent, as shown below. The one-electron Hamiltonian $\hat{h}^{\gamma}_\sigma$ contains the kinetic energy, a local potential in r space $\nu^{\gamma}_\sigma(\hat{\mathbf{r}})$ and a nonlocal exchange operator $\hat{k}^{\gamma}_\sigma$. The local r space potential is further decomposed into three contributions

$$\nu^{\gamma}_\sigma(\mathbf{r}) = \nu_{ext}(\mathbf{r}) + \nu_H(\mathbf{r}) + \nu^{\gamma}_{XC,\sigma}(\mathbf{r}), \quad (10)$$

where $\nu_H(\mathbf{r}) = \frac{\delta E_H[n]}{\delta n(\mathbf{r})} = \int n(\mathbf{r})u_C(|\mathbf{r} - \mathbf{r}'|)\,d\mathbf{r}'$ is the Hartree potential and $\nu^{\gamma}_{XC,\sigma}(\mathbf{r}) = \frac{\delta E^{\gamma}_{XC}[n]}{\delta\rho_\sigma(\mathbf{r},\mathbf{r})}$ is the short-range exchange−correlation potential. The nonlocal exchange operator $\hat{k}^{\gamma}_\sigma = \left.\frac{\delta K^{\gamma}_X}{\delta\hat{\rho}_\sigma}\right|_{[\rho^{\gamma}_\uparrow,\rho^{\gamma}_\downarrow]}$ is expressed by its operation on a wave function $\psi_\sigma(\mathbf{r})$ of the same spin as

$$\hat{k}^{\gamma}_\sigma\psi_\sigma(\mathbf{r}) = -\int u^{\gamma}_C(|\mathbf{r} - \mathbf{r}'|)\rho^{\gamma}_\sigma(\mathbf{r}, \mathbf{r}')\psi_\sigma(\mathbf{r}')\,d\mathbf{r}'. \quad (11)$$

In this work, we consider closed-shell systems where $s_z = 0$ and $N_e = 2N_H$, where N_H is the number of electron pairs, that is, the level number of the highest occupied molecular orbital (HOMO). In this case, as in Hartree−Fock theory and DFT, the DM eigenvalues $f_{j\sigma}$ that minimize $E^{\gamma}_{RSH}[\rho_\uparrow,\rho_\downarrow]$ are $f_{j,\sigma} = 1$ if $j \le N_H$ and 0 otherwise.[57] Hence, these conditions are used a priori as constraints during the minimization of $E^{\gamma}_{RSH}[\rho_\uparrow,\rho_\downarrow]$. However, for the tuning process the ensemble partial ionization of an up-spin (or down-spin) electron needs to be considered. Thus, these values for $f_{j,\sigma}$ are still used except for $j = N_H$ and $\sigma = \uparrow$, where $f_{H\uparrow}$ is fixed to be a positive fraction (i.e., the negative of the overall charge of the system, $-c$) during the minimization of the GKS ensemble energy $E^{\gamma}_{RSH}[\rho_\uparrow,\rho_\downarrow]$ (for clarity, we abbreviate $N_H \equiv H$ for the frontier orbital energy (ε) and occupation (f)). We note in passing that tuning is often done by combining a linearity condition from the $N + 1$ electron system.[58] We leave this for future work and state that it can be done along the same lines as those described here for the N-electron system.

The optimally tuned range parameter γ is determined from the requirement that the highest occupied generalized KS orbital energy $\varepsilon^{\gamma}_{H,\sigma}$ is independent of its occupancy $f_{H,\sigma}$

$$\frac{\partial\varepsilon^{\gamma}_{H,\uparrow}}{\partial f_{H,\uparrow}} = 0. \quad (12)$$

DOI: 10.1021/acs.jpca.5b10573
J. Phys. Chem. A XXXX, XXX, XXX−XXX

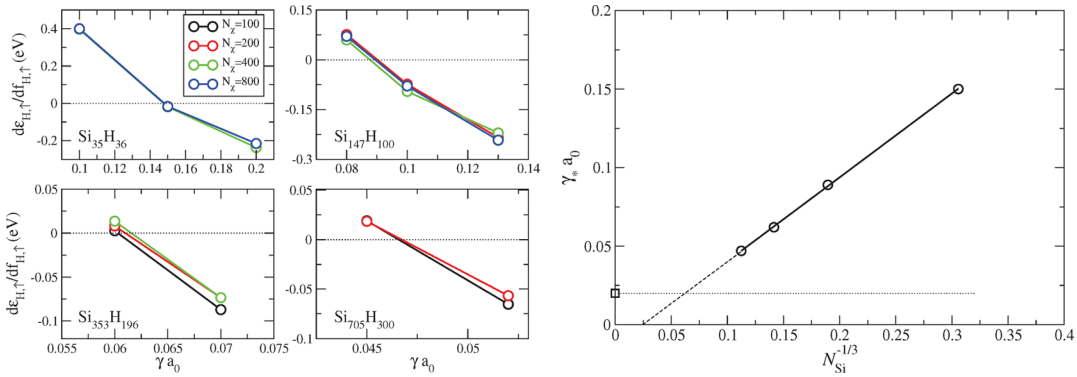

Figure 1. (Left panels) The curvature as a function of γ for the HOMO energy, $\partial\varepsilon_{H,\uparrow}/\partial f_{H,\uparrow}$ for different silicon NCs and for a different number of stochastic orbitals used to evaluate the nonlocal exchange. (Right panel) The optimal value of γ determined by eq 12 for the selected silicon NCs. The results are best-fitted to $-0.013 + 0.53N_{Si}^{-1/3}$. The square is the reverse-engineered value of γ that yields the experimental band gap of bulk silicon (ref 60).

Through Janak's theorem,[59] this equation implies that the energy curvature $\frac{\partial^2 E^{\gamma}_{RHS}}{\partial f^2_{H,\uparrow}}$ is zero. In practical terms, eq 12 is solved by a graphical root search, as shown in Figure 1 and discussed below.

STOCHASTIC FORMULATION OF THE NONLOCAL EXCHANGE OPERATOR

In real-space or plane-waves implementations, the application of the Hamiltonian $\hat{h}_{KS}$ on a single-particle wave function involves a pair of fast Fourier transforms (FFTs) to switch the wave function between k−space where the kinetic energy is applied and r−space for applying the potential energy.[61] Therefore, for a grid of N_g grid points, the operational cost is $10N_g \log_2 N_g$. The KS Hamiltonian operation scales quasilinearly with system size. The scaling is much steeper for the RSH Hamiltonian because the nonlocal exchange operator $\hat{k}^{\gamma}_{\sigma}$ applies N_e Coulomb convolution integrals, each of which is done using a FFT of its own, thus involving $10N_g \log_2 N_g \times N_e$ operations. Therefore, the GKS Hamiltonian operation, which scales quasiquadratically, is much more time-consuming than the KS Hamiltonian. Our approach, described next, reduces significantly the operation cost and even lowers the scaling due to the reduction of the optimal value of the range parameter, γ_*, as the system size grows.[62,63]

We first express the occupations in the DM in eq 4 as a combination of a occupations of a closed-shell DM and a remnant due to the overall charge of the molecule, c (assuming $-1 \le c \le 1$). This separation reduces the stochastic error later when the charge of the system is continuously varied, as needed for the optimal tuning. Thus

$$\rho_{\sigma}(\mathbf{r}, \mathbf{r}') = \sum_{j} f_{j,\sigma}\phi_{j,\sigma}(\mathbf{r})\phi^{*}_{j,\sigma}(\mathbf{r}') = \sum_{j\le N_H} \phi_{j,\sigma}(\mathbf{r})\phi^{*}_{j,\sigma}(\mathbf{r}') - c\phi_{F\uparrow}(\mathbf{r})\phi^{*}_{F\uparrow}(\mathbf{r}'), \tag{13}$$

where $\phi_{F\uparrow}$ is the frontier orbital being charged (F = H or L) and c is the amount of charge. When tuning the neutral system F = H is the HOMO, and it is being positively charged (electrons removed from HOMO); therefore, $c > 0$. When tuning for the anion, F = H + 1 is the lowest occupied molecular orbital (LUMO), and the system is negatively charged (electrons are added to the LUMO); therefore, $c < 0$.

We assume that without loss of generality, the spin of the charge frontier orbital is up. Next, we evaluate the first term on the right-hand side of eq 13 using stochastic orbitals, which are functions on the grid assigning a random sign at each grid point

$$\xi(\mathbf{r}) = \langle \mathbf{r}|\xi\rangle = \pm\frac{1}{\sqrt{h^3}}. \tag{14}$$

Stochastic orbitals offer a stochastic representation of the identity operator[64]

$$\langle|\xi\rangle\langle\xi|\rangle_{\xi} = \hat{1}. \tag{15}$$

Using this identity, just about any computation on the grid can be converted into a stochastic process.[45−50,55,65−68] For our purpose here, we define the following occupied-projected random functions on the grid ($\mathbf{r}$ is a grid point)

$$\eta_{\sigma}(\mathbf{r}) = \sum_{j\le N_H} \phi_{j,\sigma}(\mathbf{r})\langle\phi_{j,\sigma}|\xi\rangle, \tag{16}$$

where $\phi_{j,\sigma}(\mathbf{r})$ are the occupied (orthonormal) eigenstates of $\hat{h}_{\sigma}$. Then, the average of the product

$$\langle\eta_{\sigma}(\mathbf{r})\eta^{*}_{\sigma}(\mathbf{r}')\rangle_{\xi} = \sum_{j,k\le N_H} \phi_{j,\sigma}(\mathbf{r})\langle\langle\phi_{j,\sigma}|\xi\rangle\langle\xi|\phi_{k,\sigma}\rangle\rangle_{\xi}\phi^{*}_{k,\sigma}(\mathbf{r}') \tag{17}$$

can be evaluated using $\langle\langle\phi_{j,\sigma}|\xi\rangle\ \langle\xi|\phi_{k,\sigma}\rangle\rangle_{\xi} = \delta_{jk}$ (from eq 15 and the orthonormality of $\phi_{j,\sigma}(\mathbf{r})$), thus leading to the elegant stochastic representation of the DM

$$\rho_{\sigma}(\mathbf{r}, \mathbf{r}') = \langle\eta_{\sigma}(\mathbf{r})\eta^{*}_{\sigma}(\mathbf{r}')\rangle_{\xi}. \tag{18}$$

With this, eq 11 is rewritten as

$$\hat{k}^{\gamma}_{\sigma}\psi_{\sigma}(\mathbf{r}) = -\langle\eta_{\sigma}(\mathbf{r})\int u^{\gamma}_{C}(|\mathbf{r}-\mathbf{r}'|)\eta^{*}_{\sigma}(\mathbf{r}')\psi_{\sigma}(\mathbf{r}')\,d\mathbf{r}'\rangle_{\xi} + c\delta_{\sigma,\uparrow}\int u^{\gamma}_{C}(|\mathbf{r}-\mathbf{r}'|)\phi_{F,\sigma}(\mathbf{r})\phi^{*}_{F,\sigma}(\mathbf{r}')\psi_{\sigma}(\mathbf{r}')\,d\mathbf{r}'. \tag{19}$$

Next, we address the convolution in the random part of the above expression by rewriting the range-separated Coulomb potential as

$$u^{\gamma}_{C}(|\mathbf{r}-\mathbf{r}'|) = \langle\zeta(\mathbf{r})\zeta^{*}(\mathbf{r}')\rangle_{\varphi}, \tag{20}$$

where $\zeta(\mathbf{r}) = (2\pi)^{-3}\int d\mathbf{k}\sqrt{\tilde{u}^{\gamma}_{C}(\mathbf{k})}\,e^{i\varphi(\mathbf{k})}e^{i\mathbf{k}\cdot\mathbf{r}}$, $\tilde{u}^{\gamma}_{C}(\mathbf{k})$ is the Fourier transform of $u^{\gamma}_{C}(\mathbf{r})$, and $\varphi(\mathbf{k})$ is a random phase

DOI: 10.1021/acs.jpca.5b10573
J. Phys. Chem. A XXXX, XXX, XXX−XXX

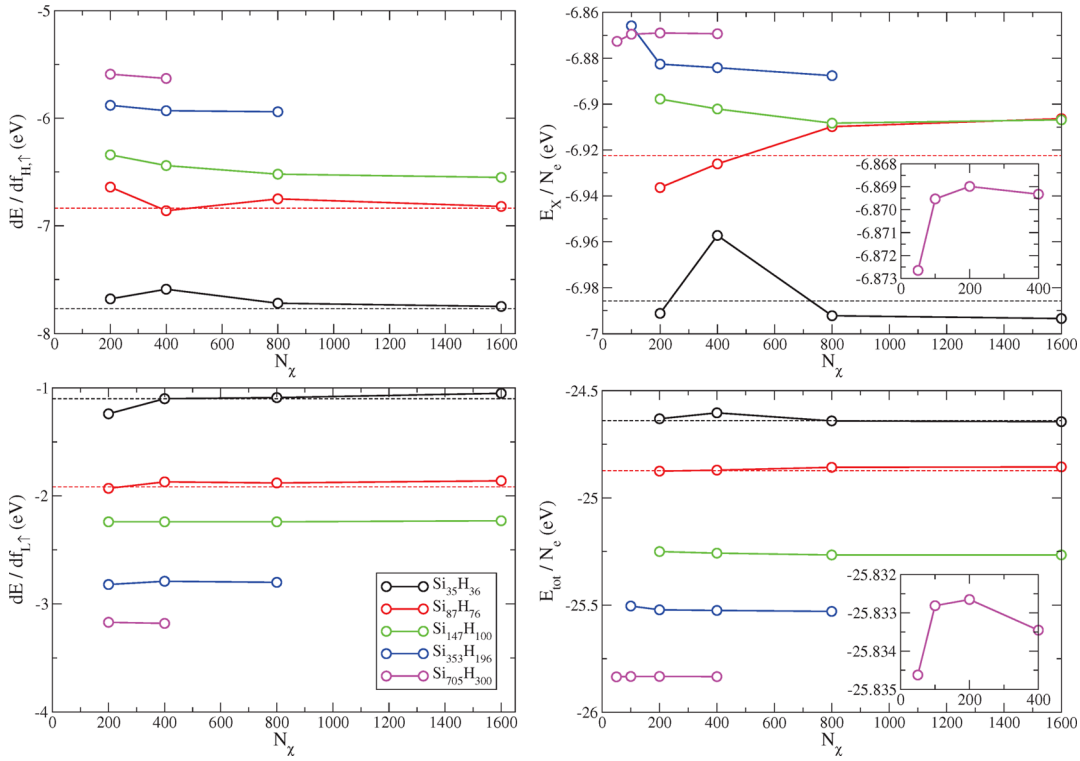

Figure 2. (Left panels) Convergence of the HOMO (H) energy (upper left panel) and the LUMO (L = H + 1) energy (lower left panel) with the number of stochastic orbitals N_χ for silicon NCs using the BNL range-separated functional. (Right panels) Convergence of the total exchange energy (upper right panel) and the total energy (lower right panel) with the number of stochastic orbitals N_χ for the corresponding silicon NCs. (Insets) A zoom of the results for the largest silicon NC, $Si_{705}H_{300}$. Dashed lines are the corresponding deterministic results where the exchange operator is calculated with all occupied orbitals using FFT for the Coulomb convolutions.

between 0 and 2π at each k space grid point. This can be seen by inserting the definition of $\zeta(\mathbf{r})$ into eq 20 and using the identity $\langle e^{-i[\varphi(\mathbf{k})-\varphi(\mathbf{k}')]}\rangle_\varphi = (2\pi)^3\delta(\mathbf{k}-\mathbf{k}')$ (see the Appendix for the treatment of the $k = 0$ term). The nonlocal exchange operation is finally written as

$$\hat{k}^\gamma_\sigma\psi_\sigma(\mathbf{r}) = -\langle\eta_\sigma(\mathbf{r})\zeta(\mathbf{r})\int\zeta^*(\mathbf{r}')\eta^*_\sigma(\mathbf{r}')\psi_\sigma(\mathbf{r}')\,d\mathbf{r}'\rangle_{\xi,\varphi} + c\delta_{\sigma,\uparrow}\int u^\gamma_C(|\mathbf{r}-\mathbf{r}'|)\phi_{F,\sigma}(\mathbf{r})\phi^*_{F,\sigma}(\mathbf{r}')\psi_\sigma(\mathbf{r}')\,d\mathbf{r}'. \quad (21)$$

In actual applications, we use a finite number N_χ of pairs of stochastic orbitals $\chi_\sigma(\mathbf{r}) = \zeta(\mathbf{r})\eta_\sigma(\mathbf{r})$, and thus

$$\hat{k}^\gamma_\sigma\psi_\sigma(\mathbf{r}) = -\frac{1}{N_\chi}\sum_\chi\chi_\sigma(\mathbf{r})\langle\chi_\sigma|\psi_\sigma\rangle + c\delta_{\sigma,\uparrow}\int u^\gamma_C(|\mathbf{r}-\mathbf{r}'|)\phi_{F,\sigma}(\mathbf{r})\phi^*_{F,\sigma}(\mathbf{r}')\psi_\sigma(\mathbf{r}')\,d\mathbf{r}'. \quad (22)$$

The $\zeta(\mathbf{r})$'s are calculated once and stored in memory, while the $\eta_\sigma(\mathbf{r})$'s are generated on the fly. The computational scaling of the nonlocal exchange operation on $\psi_\sigma(\mathbf{r})$ is thus $N_\chi N_g$ (versus $10N_g \log_2 N_g \times N_e$ for the deterministic case). Typically, N_χ = 200 and $N_g = 10^6$, and thus, the operation of the stochastic nonlocal exchange becomes comparable in terms of computational effort to that of operating with the kinetic energy; therefore, the computational cost of applying the GKS Hamiltonian is similar to that of the KS Hamiltonian.

RESULTS FOR SILICON NCS

The new method has been implemented using the BNL functional[34,35] for a series of hydrogen-passivated silicon NCs of varying sizes, $Si_{35}H_{36}$, $Si_{87}H_{76}$, $Si_{147}H_{100}$, $Si_{353}H_{196}$, and $Si_{705}H_{300}$, with real-space grids of 60^3, 64^3, 70^3, 90^3, and 108^3 grid points, respectively. We solve the generalized KS equations fully self-consistently using the Chebyshev-filtered subspace acceleration[69,70] to obtain the occupied and low-lying unoccupied eigenfunctions and eigenvalues.

The energy curvature for the different NCs is estimated from the forward difference formula concerning the HOMO energy $-\frac{\partial\varepsilon_{H,\uparrow}(c)}{\partial c} \approx \frac{\varepsilon_{H,\uparrow}(0)-\varepsilon_{H,\uparrow}(\delta)}{\delta}$, with $\delta = 0.125$, is plotted as a function of γ in Figure 1. The curvature is a decreasing function of γ and has a node at the optimal value of the range parameter γ_*. When $\gamma < \gamma_*$ ($\gamma > \gamma_*$), the curvature is positive (negative), and we have delocalization (localization) errors.[71] For each NC, the curvature results are shown for several values of the number of stochastic orbitals N_χ. We find that the statistical fluctuations near γ_* become smaller as the system grows and can be reduced with proper choice of N_χ. For example, for the larger system, the results near γ_* can be converged with only $N_\chi \approx 200$ compared to the total number of occupied states for this system, which is 1560. The reduction of these fluctuations is partially due to the decrease of γ_* itself as the NC size increases (this decrease is shown in the right panel of Figure 1), leading to a smaller contribution of the nonlocal exchange to the orbital energies.

The results in the right panel of the figure also show that γ_* closely follows a linear function of $N_{Si}^{-1/3}$. We expect that for larger NCs with $N_{Si} > 2500$, this linear relation will break down,

DOI: 10.1021/acs.jpca.5b10573
J. Phys. Chem. A XXXX, XXX, XXX−XXX

and the optimal range parameter will converge to the bulk value, which through reverse engineering[60] can be estimated as $\gamma_*^\infty = 0.02a_0^{-1}$ (shown as a horizontal dotted line). Such a localization induced by the exchange has been seen for 1D conjugated polymers[72] but not for bulk solids like silicon, likely due to the enormity of the calculation.

In Figure 2, we plot the HOMO (upper left panel) and the LUMO (lower left panel) energies, the total exchange energy per electron (upper right panel), and the total energy per electron (lower right panel). The HOMO and LUMO orbital energies were obtained from the relations[59]

$$\varepsilon_{H,\uparrow} = -\left.\frac{\partial E_{RSH}^{\gamma}[\rho_\uparrow, \rho_\downarrow]}{\partial c}\right|_{c\to 0^+}$$
$$\varepsilon_{L,\uparrow} = -\left.\frac{\partial E_{RSH}^{\gamma}[\rho_\uparrow, \rho_\downarrow]}{\partial c}\right|_{c\to 0^-} \quad (23)$$

respectively, as a function of N_χ at γ_*. We find that determining the HOMO and LUMO energies using the above first derivative relations reduces the noise compared to obtaining their values directly from the eigenvalues. Clearly $\varepsilon_{H,\uparrow}$, $\varepsilon_{L,\uparrow}$ and the total exchange and total energies per electron converge as N_χ increases. As the system size increases, the fluctuations in $\varepsilon_{H,\uparrow}$ and $\varepsilon_{L,\uparrow}$ decrease for a given value of N_χ, consistent with the discussion above. This is evident from the plot of the differences between the frontier orbital energies at adjacent values of N_χ. A similar conclusion can be drawn for the total exchange energy and total energy per electron. The insets in the right panels show that for the largest systems studied, the fluctuations in these quantities are a few meV's. This is sufficient to converge the quasiparticle energies of the frontier orbitals to within an experimental relevant accuracy; however, note that the statistical fluctuation in the total energy itself is still rather large (≈1 eV).

Turning to compare the current results with the stochastic GW approach,[45] in the lower panel of Figure 3, we plot the converged (with respect to N_χ) HOMO and LUMO energies at γ_* for the series of silicon NCs. For the two smallest systems ($Si_{35}H_{36}$ and $Si_{87}H_{76}$), we compare the stochastic approach

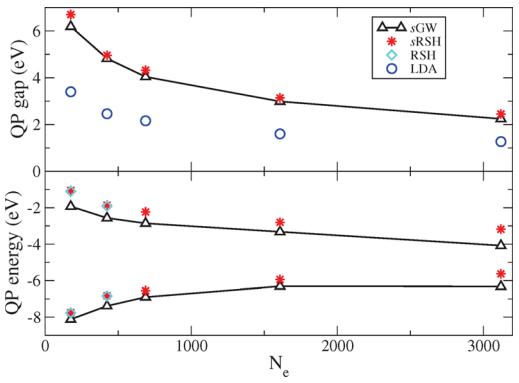

Figure 3. (Lower panel) Comparison of the HOMO and LUMO energies obtained using the sGW approach (black triangles) and the stochastic RSH within the BNL functional (red asterisk) for a series of silicon NCs. The cyan diamond represents the deterministic RSH within the BNL functional. (Upper panel) The corresponding quasiparticle band gaps. Also shown is the DFT result within the LDA (blue circles).

developed here with a deterministic RSH calculation using all occupied orbitals for the range-separated exchange and obtain the Coulomb convolution integrals with FFTs, thereby eliminating any source of statistical error. The purpose is to show that when the stochastic results are converged, the agreement with a deterministic calculations is perfect on a relevant magnitude of energy. We find that the HOMO energy increases and the LUMO energy decreases with the size of the NC. This is consistent with our recent calculations on silicon NCs using the stochastic GW approach, albeit with the fact that there is a small shift in the quasiparticle energies obtained from the stochastic RSH approach compared to the sGW. Indeed, a similar shift has been reported previously for much smaller silicon NCs.[40] However, the source of this discrepancy is not clear, particularly because the GW calculations were done within the so-called G_0W_0 limit, and the OT-RSH often provides better quasiparticle energies in comparison to experiments.[41] In the upper panel of Figure 3, we plot the fundamental (quasiparticle) gaps. Here, the agreement with the sGW approach is rather remarkable, especially compared to the LDA results, which significantly underestimate the quasiparticle gap across all sizes studied.

In Table 1, we provide numerical details of the calculations for the smallest and largest NC studied. We report the results

Table 1. Optimally Tuned BNL Frontier Orbital Energies and Computational Times T_{CPU} versus the Number of Stochastic Orbitals N_χ for Two (Medium and Large) Silicon Clusters. Values for LDA Are Also Given for Comparison as the System Size Grows, T_{CPU} for the Optimally Tuned BNL Decreases Relative to the LDA Timings Due to a Decrease of γ_*[a]

system	functional	N_χ	ε_H (eV)	ε_L (eV)	ε_g (eV)	T_{CPU}[d]
$Si_{35}H_{36}$	LDA		−6.13	−2.73	3.40	1.6
	BNL[b]	800	−7.72	−1.09	6.63	16
		1600	−7.75	−1.05	6.70	30
$Si_{705}H_{300}$	LDA		−5.13	−3.85	1.28	132
	BNL[c]	200	−5.59	−3.18	2.41	234
		400	−5.63	−3.17	2.46	310

[a]As the system size grows, T_{CPU} for the optimally tuned BNL decreases relative to the LDA timings due to a decrease of γ_*. [b]$\gamma_* = 0.148\ a_0^{-1}$. [c]$\gamma_* = 0.047\ a_0^{-1}$. [d]In CPU hours.

for the HOMO and LUMO orbital energies for two different choices of N_χ. Comparing these two values, we can conclude that the statistical errors for the LUMO are very small (≈0.01 eV) for the largest NC, and even the HOMO has small errors of around ∼0.05 eV. Moreover, similar or even larger statistical errors are observed for the smaller NC for much larger values of N_χ, indicating that for a given accuracy, the number of stochastic orbitals decreases with the system size. This is partially correlated with the reduction of γ_* with the system size, as discussed above.

SUMMARY

We have developed a stochastic representation for the nonlocal exchange operator in order to combine real-space/plane-waves methods with OT-RSH functionals within the generalized Kohn−Sham scheme. Our formalism uses two principles: one is a stochastic decomposition of the Coulomb convolution integrals, and the other is the representation of the DM using stochastic orbitals. Combining these two ideas leads to a

DOI: 10.1021/acs.jpca.5b10573
J. Phys. Chem. A XXXX, XXX, XXX−XXX

significant reduction of the computational effort and, for the systems studied in this work, to a reduction of the computational scaling of the nonlocal exchange operator, at the price of introducing a statistical error. The statistical error is controlled by increasing the number of stochastic orbitals and is also found to reduce as system size grows. Applications to silicon NCs of varying sizes show relatively good agreement for the band edge quasiparticle excitations in comparison to a many-body perturbation approach within the sGW approximation and excellent agreement for the fundamental band gap. The stochastic approach has a major advantage over the sGW by providing a self-consistent Hamiltonian that is central for postprocessing, for example, in conjunction with a real-time Bethe–Salpeter approach.[55] The results shown here for $N_e > 3000$ and $N_g > 10^6$ are the largest reported so far for the optimally tuned range-separated generalized Kohn–Sham approach.

APPENDIX: TREATMENT OF THE $K = 0$ TERM

For accelerating convergence, it turns out to be better to remove the $\tilde{u}_C^\gamma(\mathbf{k}=0)$ term from the random vector expression representing the interaction, that is

$$\zeta(\mathbf{r}) = (2\pi)^{-3} d\mathbf{k} \sum_{\mathbf{k}\neq\mathbf{0}} \sqrt{\tilde{u}_C^\gamma(\mathbf{k})}\, e^{i\varphi(\mathbf{k})} e^{i\mathbf{k}\cdot\mathbf{r}}.$$

This is because in practice, the $\tilde{u}_C^\gamma(\mathbf{k}=0)$ term is very large. Analytically, this term is easily shown to commute with the Fock Hamiltonian and simply contribute a constant (times the occupation) to the eigenvalues and to the total energy; therefore, it can be added a posteriori

$$\hat{k}_\sigma^\gamma \phi_{j,\sigma}(\mathbf{r}) \rightarrow \hat{k}_\sigma^\gamma \phi_{j,\sigma}(\mathbf{r}) - f_{j,\sigma} \nu_{0X} \phi_{j,\sigma}(\mathbf{r})$$

$$\varepsilon_{j,\sigma}^\gamma \rightarrow \varepsilon_{j,\sigma}^\gamma - f_{j,\sigma} \nu_{0X}$$

$$K[\rho_\uparrow, \rho_\downarrow] \rightarrow K[\rho_\uparrow, \rho_\downarrow] - \frac{1}{2} \nu_{0X} \sum f_{j\sigma}^2,$$

where

$$\nu_{0X} \equiv (2\pi)^{-3} d\mathbf{k} \tilde{u}_C^\gamma(\mathbf{k} = \mathbf{0}).$$

AUTHOR INFORMATION

Corresponding Authors

*E-mail: dxn@chem.ucla.edu (D.N.).
*E-mail: eran.rabani@berkeley.edu (E.R.).
*E-mail: roi.baer@huji.ac.il (R.B.).

Present Address

‖R.B.: On Sabbatical leave at the Department of Chemistry, University of California, Berkeley, California 94720, United States.

Notes

The authors declare no competing financial interest.

ACKNOWLEDGMENTS

R.B. and E.R. gratefully thank the Israel Science Foundation–FIRST Program (Grant No. 1700/14). R.B. gratefully acknowledges support for his sabbatical visit by the Pitzer Center and the Kavli Institute of the University of California, Berkeley. D.N. and E.R. acknowledge support by the NSF, Grants CHE-1112500 and CHE-1465064, respectively. We dedicate this paper to Prof. Ronnie Kosloff from the Hebrew University to acknowledge his important contributions to the field of computational/theoretical chemistry. Kosloff has been our teacher and mentor for many years and his methods, such as the Chebyshev expansions and Fourier grids, were used extensively in our present work as well.

REFERENCES

(1) Kohn, W.; Sham, L. J. Self-Consistent Equations Including Exchange and Correlation Effects. *Phys. Rev.* **1965**, *140*, A1133.
(2) Öğüt, S.; Chelikowsky, J. R.; Louie, S. G. Quantum Confinement and Optical Gaps in Si Nanocrystals. *Phys. Rev. Lett.* **1997**, *79*, 1770–1773.
(3) Godby, R. W.; White, I. D. Density-Relaxation Part of the Self-Energy. *Phys. Rev. Lett.* **1998**, *80*, 3161–3161.
(4) Teale, A. M.; De Proft, F.; Tozer, D. J. Orbital Energies and Negative Electron Affinities From Density Functional Theory: Insight From the Integer Discontinuity. *J. Chem. Phys.* **2008**, *129*, 044110–12.
(5) Almbladh, C.-O.; von Barth, U. Exact Results for the Charge and Spin Densities, Exchange-Correlation Potentials, and Density-Functional Eigenvalues. *Phys. Rev. B: Condens. Matter Mater. Phys.* **1985**, *31*, 3231–3244.
(6) Perdew, J. P.; Parr, R. G.; Levy, M.; Balduz, J. L. Density functional theory for fractional particle number: Derivative discontinuities of the energy. *Phys. Rev. Lett.* **1982**, *49*, 1691–1694.
(7) Sham, L. J.; Schlüter, M. Density Functional Theory of the Gap. *Phys. Rev. Lett.* **1983**, *51*, 1888–1891.
(8) Hedin, L. New Method for Calculating the One-Particle Green's Function with Application to the Electron-Gas Problem. *Phys. Rev.* **1965**, *139*, A796–A823.
(9) Friedrich, C.; Schindlmayr, A. In Many-Body Perturbation Theory: The GW Approximation. *Computational Neuroscience: Do It Yourself*; Grotendorst, S., Blügel, D. M., Eds.; NIC Series; John von Neumann Institute for Computing: Julich, Germany; 200631335345
(10) Hybertsen, M. S.; Louie, S. G. First-Principles Theory of Quasiparticles: Calculation of Band Gaps in Semiconductors and Insulators. *Phys. Rev. Lett.* **1985**, *55*, 1418–1421.
(11) Del Sole, R.; Reining, L.; Godby, R. GWΓ Approximation for Electron Self-Energies in Semiconductors and Insulators. *Phys. Rev. B: Condens. Matter Mater. Phys.* **1994**, *49*, 8024–8028.
(12) Steinbeck, L.; Rubio, A.; Reining, L.; Torrent, M.; White, I.; Godby, R. Enhancements To the GW Space-Time Method. *Comput. Phys. Commun.* **1999**, *125*, 05–118.
(13) Fleszar, A. LDA, GW, and Exact-Exchange Kohn–Sham Scheme Calculations of the Electronic Structure of Sp Semiconductors. *Phys. Rev. B: Condens. Matter Mater. Phys.* **2001**, *64*, 245204.
(14) Onida, G.; Reining, L.; Rubio, A. Electronic Excitations: Density-Functional Versus Many-Body Green's-Function Approaches. *Rev. Mod. Phys.* **2002**, *74*, 601–659.
(15) Rinke, P.; Qteish, A.; Neugebauer, J.; Freysoldt, C.; Scheffler, M. Combining GW Calculations With Exact-Exchange Density-Functional Theory: An Analysis of Valence-Band Photoemission for Compound Semiconductors. *New J. Phys.* **2005**, *7*, 126.
(16) Shishkin, M.; Kresse, G. Self-Consistent GW Calculations for Semiconductors and Insulators. *Phys. Rev. B: Condens. Matter Mater. Phys.* **2007**, *75*, 235102.
(17) Trevisanutto, P. E.; Giorgetti, C.; Reining, L.; Ladisa, M.; Olevano, V. Ab Initio GW Many-Body Effects in Graphene. *Phys. Rev. Lett.* **2008**, *101*, 226405.
(18) Rostgaard, C.; Jacobsen, K. W.; Thygesen, K. S. Fully Self-Consistent GW Calculations for Molecules. *Phys. Rev. B: Condens. Matter Mater. Phys.* **2010**, *81*, 085103.
(19) Liao, P.; Carter, E. A. Testing Variations of the GW Approximation On Strongly Correlated Transition Metal Oxides: Hematite (α-Fe2o3) As A Benchmark. *Phys. Chem. Chem. Phys.* **2011**, *13*, 15189–15199.
(20) Blase, X.; Attaccalite, C.; Olevano, V. First-Principles GW Calculations for Fullerenes, Porphyrins, Phtalocyanine, and Other

DOI: 10.1021/acs.jpca.5b10573
J. Phys. Chem. A XXXX, XXX, XXX–XXX

Molecules of Interest for Organic Photovoltaic Applications. *Phys. Rev. B: Condens. Matter Mater. Phys.* **2011**, *83*, 115103.
(21) Tamblyn, I.; Darancet, P.; Quek, S. Y.; Bonev, S. A.; Neaton, J. B. Electronic Energy Level Alignment At Metal-Molecule Interfaces With A GW Approach. *Phys. Rev. B: Condens. Matter Mater. Phys.* **2011**, *84*, 201402.
(22) Samsonidze, G.; Jain, M.; Deslippe, J.; Cohen, M. L.; Louie, S. G. Simple Approximate Physical Orbitals for GW Quasiparticle Calculations. *Phys. Rev. Lett.* **2011**, *107*, 186404.
(23) Marom, N.; Caruso, F.; Ren, X.; Hofmann, O. T.; Körzdörfer, T.; Chelikowsky, J. R.; Rubio, A.; Scheffler, M.; Rinke, P. Benchmark of GW Methods for Azabenzenes. *Phys. Rev. B: Condens. Matter Mater. Phys.* **2012**, *86*, 245127.
(24) van Setten, M.; Weigend, F.; Evers, F. The GW-Method for Quantum Chemistry Applications: Theory and Implementation. *J. Chem. Theory Comput.* **2013**, *9*, 232−246.
(25) Pham, T. A.; Nguyen, H.-V.; Rocca, D.; Galli, G. GW Calculations Using the Spectral Decomposition of the Dielectric Matrix: Verification, Validation, and Comparison of Methods. *Phys. Rev. B: Condens. Matter Mater. Phys.* **2013**, *87*, 155148.
(26) Seidl, A.; Görling, A.; Vogl, P.; Majewski, J. A.; Levy, M. Generalized Kohn-Sham Schemes and the Band-Gap Problem. *Phys. Rev. B: Condens. Matter Mater. Phys.* **1996**, *53*, 3764−3774.
(27) Heyd, J.; Peralta, J. E.; Scuseria, G. E.; Martin, R. L. Energy Band Gaps and Lattice Parameters Evaluated With the Heyd-Scuseria-Ernzerhof Screened Hybrid Functional. *J. Chem. Phys.* **2005**, *123*, 174101.
(28) Gerber, I. C.; Angyan, J. G.; Marsman, M.; Kresse, G. Range Separated Hybrid Density Functional With Long-Range Hartree-Fock Exchange Applied To Solids. *J. Chem. Phys.* **2007**, *127*, 054101.
(29) Brothers, E. N.; Izmaylov, A. F.; Normand, J. O.; Barone, V.; Scuseria, G. E. Accurate Solid-State Band Gaps Via Screened Hybrid Electronic Structure Calculations. *J. Chem. Phys.* **2008**, *129*, 011102.
(30) Barone, V.; Hod, O.; Peralta, J. E.; Scuseria, G. E. Accurate Prediction of the Electronic Properties of Low-Dimensional Graphene Derivatives Using a Screened Hybrid Density Functional. *Acc. Chem. Res.* **2011**, *44*, 269−279.
(31) Savin, A.; Flad, H. J. Density Functionals for the Yukawa Electron-Electron Interaction. *Int. J. Quantum Chem.* **1995**, *56*, 327−332.
(32) Iikura, H.; Tsuneda, T.; Yanai, T.; Hirao, K. A Long-Range Correction Scheme for Generalized-Gradient-Approximation Exchange Functionals. *J. Chem. Phys.* **2001**, *115*, 3540−3544.
(33) Yanai, T.; Tew, D. P.; Handy, N. C. A New Hybrid Exchange-Correlation Functional Using the Coulomb-Attenuating Method (Cam-B3lyp). *Chem. Phys. Lett.* **2004**, *393*, 51−57.
(34) Baer, R.; Neuhauser, D. A Density Functional Theory With Correct Long-Range Asymptotic Behavior. *Phys. Rev. Lett.* **2005**, *94*, 043002.
(35) Livshits, E.; Baer, R. A Well-Tempered Density Functional Theory of Electrons in Molecules. *Phys. Chem. Chem. Phys.* **2007**, *9*, 2932−2941.
(36) Vydrov, O. A.; Scuseria, G. E. Assessment of A Long-Range Corrected Hybrid Functional. *J. Chem. Phys.* **2006**, *125*, 234109.
(37) Chai, J. D.; Head-Gordon, M. Long-Range Corrected Hybrid Density Functionals With Damped Atom-Atom Dispersion Corrections. *Phys. Chem. Chem. Phys.* **2008**, *10*, 6615−6620.
(38) Livshits, E.; Baer, R. A Density Functional Theory for Symmetric Radical Cations from Bonding to Dissociation. *J. Phys. Chem. A* **2008**, *112*, 12789−12791.
(39) Baer, R.; Livshits, E.; Salzner, U. Tuned Rannge-Separated Hybrids in Density Functional Theory. *Annu. Rev. Phys. Chem.* **2010**, *61*, 85−109.
(40) Stein, T.; Eisenberg, H.; Kronik, L.; Baer, R. Fundamental Gaps of Finite Systems From the Eigenvalues of A Generalized Kohn-Sham Method. *Phys. Rev. Lett.* **2010**, *105*, 266802.
(41) Kronik, L.; Stein, T.; Refaely-Abramson, S.; Baer, R. Excitation Gaps of Finite-Sized Systems from Optimally Tuned Range-Separated Hybrid Functionals. *J. Chem. Theory Comput.* **2012**, *8*, 1515−1531.
(42) Körzdörfer, T.; Parrish, R. M.; Marom, N.; Sears, J. S.; Sherrill, C. D.; Brédas, J.-L. Assessment of the Performance of Tuned Range-Separated Hybrid Density Functionals in Predicting Accurate Quasiparticle Spectra. *Phys. Rev. B: Condens. Matter Mater. Phys.* **2012**, *86*, 205110.
(43) Jacquemin, D.; Moore, B.; Planchat, A.; Adamo, C.; Autschbach, J. Performance of an Optimally Tuned Range-Separated Hybrid Functional for 0−0 Electronic Excitation Energies. *J. Chem. Theory Comput.* **2014**, *10*, 1677−1685.
(44) Stein, T.; Autschbach, J.; Govind, N.; Kronik, L.; Baer, R. Curvature and Frontier Orbital Energies in Density Functional Theory. *J. Phys. Chem. Lett.* **2012**, *3*, 3740−3744.
(45) Neuhauser, D.; Gao, Y.; Arntsen, C.; Karshenas, C.; Rabani, E.; Baer, R. Breaking the theoretical scaling limit for predicting quasiparticle energies: the stochastic GW approach. *Phys. Rev. Lett.* **2014**, *113*, 076402.
(46) Baer, R.; Neuhauser, D.; Rabani, E. Self-Averaging Stochastic Kohn-Sham Density-Functional Theory. *Phys. Rev. Lett.* **2013**, *111*, 106402.
(47) Neuhauser, D.; Baer, R.; Rabani, E. Embedded Fragment Stochastic Density Functional Theory. *J. Chem. Phys.* **2014**, *141*, 041102.
(48) Baer, R.; Rabani, E. Expeditious Stochastic Calculation of Multiexciton Generation Rates in Semiconductor Nanocrystals. *Nano Lett.* **2012**, *12*, 2123−2127.
(49) Neuhauser, D.; Rabani, E.; Baer, R. Expeditious Stochastic Approach for MP2 Energies in Large Electronic Systems. *J. Chem. Theory Comput.* **2013**, *9*, 24−27.
(50) Neuhauser, D.; Rabani, E.; Baer, R. Expeditious Stochastic Calculation of Random-Phase Approximation Energies for Thousands of Electrons in Three Dimensions. *J. Phys. Chem. Lett.* **2013**, *4*, 1172−1176.
(51) Ge, Q.; Gao, Y.; Baer, R.; Rabani, E.; Neuhauser, D. A Guided Stochastic Energy-Domain Formulation of the Second Order Møller-Plesset Perturbation Theory. *J. Phys. Chem. Lett.* **2014**, *5*, 185−189.
(52) Gao, Y.; Neuhauser, D.; Baer, R.; Rabani, E. Sublinear Scaling for Time-Dependent Stochastic Density Functional Theory. *J. Chem. Phys.* **2015**, *142*, 034106.
(53) Baer, R.; Neuhauser, D. Communication: Monte Carlo Calculation of the Exchange Energy. *J. Chem. Phys.* **2012**, *137*, 051103−4.
(54) Cytter, Y.; Neuhauser, D.; Baer, R. Metropolis Evaluation of the Hartree-Fock Exchange Energy. *J. Chem. Theory Comput.* **2014**, *10*, 4317−4323.
(55) Rabani, E.; Baer, R.; Neuhauser, D. Time-dependent Stochastic Bethe-Salpeter Approach. *Phys. Rev. B: Condens. Matter Mater. Phys.* **2015**, *91*, 235302.
(56) Savin, A. In *Recent Advances in Density Functional Methods Part I*; Chong, D. P., Ed.; World Scientific: Singapore, 1995; p 129.
(57) Dreizler, R. M.; Gross, E. K. U. *Density Functional Theory: An Approach to the Quantum Many Body Problem*; Springer: Berlin, Germany, 1990.
(58) Stein, T.; Kronik, L.; Baer, R. Reliable Prediction of Charge Transfer Excitations in Molecular Complexes Using Time-Dependent Density Functional Theory. *J. Am. Chem. Soc.* **2009**, *131*, 2818−2820.
(59) Janak, J. Proof That [Partial] E/[Partial] Ni= Epsilon in Density-Functional Theory. *Phys. Rev. B: Condens. Matter Mater. Phys.* **1978**, *18*, 7165−7168.
(60) Eisenberg, H. R.; Baer, R. A New Generalized Kohn-Sham Method for Fundamental Band-Gaps in Solids. *Phys. Chem. Chem. Phys.* **2009**, *11*, 4674−4680.
(61) Kosloff, D.; Kosloff, R. A Fourier Method Solution for the Time-Dependent Schrodinger-Equation as a Tool in Molecular-Dynamics. *J. Comput. Phys.* **1983**, *52*, 35−53.
(62) Körzdörfer, T.; Sears, J. S.; Sutton, C.; Bredas, J.-L. Long-Range Corrected Hybrid Functionals for Pi-Conjugated Systems: Dependence of the Range-Separation Parameter On Conjugation Length. *J. Chem. Phys.* **2011**, *135*, 204107−6.

DOI: 10.1021/acs.jpca.5b10573
J. Phys. Chem. A XXXX, XXX, XXX−XXX

(63) Vlček, V.; Eisenberg, H. R.; Steinle-Neumann, G.; Kronik, L.; Baer, R. Deviations From Piecewise Linearity in the Solid-State Limit With Approximate Density Functionals. *J. Chem. Phys.* **2015**, *142*, 034107.
(64) Hutchinson, M. F. A Stochastic Estimator of the Trace of the Influence Matrix for Laplacian Smoothing Splines. *Communications in Statistics-Simulation and Computation* **1990**, *19*, 433−450.
(65) Wang, L. W. Calculating the Density-of-States and Optical-Absorption Spectra of Large Quantum-Systems by the Plane-Wave Moments Method. *Phys. Rev. B: Condens. Matter Mater. Phys.* **1994**, *49*, 10154−10158.
(66) Drabold, D. A.; Sankey, O. F. Maximum-Entropy Approach for Linear Scaling in the Electronic- Structure Problem. *Phys. Rev. Lett.* **1993**, *70*, 3631−3634.
(67) Baer, R.; Seideman, T.; Ilani, S.; Neuhauser, D. Ab Initio Study of the Alternating Current Impedance of A Molecular Junction. *J. Chem. Phys.* **2004**, *120*, 3387−3396.
(68) Baer, R.; Rabani, E. Communication: Biexciton generation rates in CdSe nanorods are length independent. *J. Chem. Phys.* **2013**, *138*, 051102−4.
(69) Zhou, Y.; Saad, Y.; Tiago, M. L.; Chelikowsky, J. R. Parallel Self-Consistent-Field Calculations Via Chebyshev-Filtered Subspace Acceleration. *Phys. Rev. E* **2006**, *74*, 066704.
(70) Khoo, K.; Kim, M.; Schofield, G.; Chelikowsky, J. R. Ab Initio Molecular Dynamics Simulations Using A Chebyshev-Filtered Subspace Iteration Technique. *Phys. Rev. B: Condens. Matter Mater. Phys.* **2010**, *82*, 064201.
(71) Mori-Sanchez, P.; Cohen, A. J.; Yang, W. T. Localization and Delocalization Errors in Density Functional Theory and Implications for Band-Gap Prediction. *Phys. Rev. Lett.* **2008**, *100*, 146401.
(72) Vlček, V.; Eisenberg, H. R.; Steinle-Neumann, G.; Baer, R. Spontaneous Charge Carrier Localization in Extended One-Dimensional Systems. arXiv preprint arXiv:1509.05222, 2015.

DOI: 10.1021/acs.jpca.5b10573
J. Phys. Chem. A XXXX, XXX, XXX−XXX